Stabilized Finite Element Methods for a Blood Flow Model of Arteriosclerosis

Feifei Jing,[1] **Jian Li,**[2] **Zhangxin Chen**[1,3]

[1] *College of Mathematics and Statistics, Center for Computational Geoscience, Xi'an Jiaotong University, Xi'an 710049, People's Republic of China*

[2] *Institute of Computational Mathematics and its Applications, Baoji University of Arts and Sciences, Baoji 721013, People's Republic of China*

[3] *Department of Chemical and Petroleum Engineering, Schulich School of Engineering, University of Calgary, 2500 University Drive N.W. Calgary, Alberta T2N 1N4, Canada*

Received 23 June 2014; revised 3 November 2014; accepted 11 February 2015
Published online 21 September 2015 in Wiley Online Library (wileyonlinelibrary.com).
DOI 10.1002/num.22005

In this article, a blood flow model of arteriosclerosis, which is governed by the incompressible Navier–Stokes equations with nonlinear slip boundary conditions, is constructed and analyzed. By means of suitable numerical integration approximation for the nonlinear boundary term in this model, a discrete variational inequality for the model based on $\mathbf{P}_1 - P_1/P_0$ stabilized finite elements is proposed. Optimal order error estimates are obtained. Finally, numerical examples are shown to demonstrate the validity of the theoretical analysis and the efficiency of the presented methods. © 2015 Wiley Periodicals, Inc. Numer Methods Partial Differential Eq 31: 2063–2079, 2015

Keywords: error estimates; Navier–Stokes equations; nonlinear slip boundary; stabilized method; variational inequality

I. INTRODUCTION

In this article, we will consider the blood flow of arteriosclerosis, which is governed by the following steady incompressible Navier–Stokes equations:

$$\begin{cases} -\nu\Delta\mathbf{u} + (\mathbf{u}\cdot\nabla)\mathbf{u} + \nabla p = \mathbf{f} & \text{in} \quad \Omega, \\ \operatorname{div}\mathbf{u} = 0 & \text{in} \quad \Omega, \end{cases} \tag{1.1}$$

where $\mathbf{u}$, p, and $\mathbf{f}$ represent the velocity vector, pressure, and prescribed body force, respectively. $\nu > 0$ stands for the viscosity coefficient of the fluid, and $\Omega \subset R^2$ is an open bounded convex

Correspondence to: Zhangxin Chen, College of Mathematics and Statistics, Center for Computational Geoscience, Xi'an Jiaotong University, Xi'an 710049, People's Republic of China (e-mail: zhachen@ucalgary.ca)
Contract grant sponsor: NSF of China; contract grant number: 11371031 and 11371288
Contract grant sponsor: The NCET-11-1041, the Key Project of Baoji university of Arts and Sciences; contract grant number: ZK15040

polygon with sufficiently smooth boundary $\partial\Omega$. Moreover, the nonlinear slip boundary conditions of friction type are presented as follows:

$$\begin{cases} \mathbf{u} = 0 & \text{on } \Gamma_D, \\ u_{\mathbf{n}} = 0, \quad |\sigma_{\boldsymbol{\tau}}| \le g, \qquad \sigma_{\boldsymbol{\tau}} u_{\boldsymbol{\tau}} + g|u_{\boldsymbol{\tau}}| = 0 & \text{on } \Gamma_S, \end{cases} \tag{1.2}$$

where $\partial\Omega = \overline{\Gamma}_D \cup \overline{\Gamma}_S$. We impose the adhesive boundary condition on Γ_D but a slip and non-leak boundary condition on Γ_S. Assume that Γ_S is not empty, whereas Γ_D may be empty, where $\Gamma_D \cap \Gamma_S = \emptyset$. Here and what follows, the unit outward normal to the boundary is denoted by $\mathbf{n}$ and $\boldsymbol{\tau}$ denotes the unit tangent vector which can be obtained by rotating $\mathbf{n}$ counterclockwise for 90°; if $\mathbf{v}$ is a vector defined on the boundary, $v_{\mathbf{n}} \equiv \mathbf{v} \cdot \mathbf{n}$ and $v_{\boldsymbol{\tau}} \equiv \mathbf{v} \cdot \boldsymbol{\tau}$ denote the normal and tangential components of $\mathbf{v}$, respectively. The function $\sigma_{\boldsymbol{\tau}} = \nu \frac{\partial u_{\boldsymbol{\tau}}}{\partial \mathbf{n}}$ is the tangential component of the stress vector defined on Γ_S. g as a strictly positive function on Γ_S is called the modulus of friction and assumed to be continuous on $\overline{\Gamma}_S$. This type of boundary conditions can be found in [1, 2] where the authors studied the blood flow in a vein of an arteriosclerosis patient.

For the slip boundary conditions (1.2), Fujita in [2] showed existence and uniqueness of a weak solution to the Stokes problem. Subsequently, Saito in [3] obtained regularity of the weak solution by Yoshida's regularized method and difference quotients. For numerical methods for the Navier–Stokes equations, Li and Li in [4] studied the pressure stabilized finite element method for this type of boundary conditions, where they treated this problem as an elliptic variational inequality of a tuple $(\mathbf{u}, p)$, which they regarded as just one variable; a theoretical analysis on convergence of a Uzawa algorithm was proved for the continuous problem in [5]. Kashiwabara in [6, 7] gave a discrete variational inequality for the Stokes equations with slip and leak boundary conditions of friction type. Other theoretical and numerical results for the steady and unsteady Stokes/Navier–Stokes problems with such boundary conditions can be found in [8–19].

Although there are a lot of theoretical analyses in the literature, it has been difficult to perform a numerical analysis for finite element methods for the blood flow model presented here. In [6], a finite element approximation for the Stokes equations of this type was discussed based on the Hood–Taylor finite element pair. In our work, we apply an equivalent variational problem [6], which is different from [4], and the Uzawa method is directly applied to a discrete problem instead of the continuous one. Furthermore, we choose the lower-order finite element pairs for the presented model. Optimal error estimates for approximate velocity and pressure are obtained. Finally, a series of numerical examples are given to illustrate the theoretical results.

This article is organized as follows: In the next section, we will introduce some notation and recall some preliminary results for the blood flow model. The continuous weak variational forms are also shown. In Section III, a stabilized finite element framework for the Navier–Stokes equations and several technical lemmas are given. Section IV is devoted to the study of optimal error estimates. In the final section, some numerical experiments are performed to validate our theoretical results developed in the previous section.

II. PRELIMINARIES

In this section, we state some notation. Let $H_0^1(\Omega)$ be the standard Sobolev space [20] equipped with the usual norm $\|\cdot\|_1$ and seminorm $|\cdot|_1$. The proper function spaces are given as follows:

$$\mathbf{V} = \{\mathbf{v} \in [H^1(\Omega)]^2 : \mathbf{v}|_{\Gamma_D} = 0, v_{\mathbf{n}}|_{\Gamma_S} = 0\}, \mathbf{V}_\sigma = \{\mathbf{v} \in \mathbf{V} : \operatorname{div} \mathbf{v} = 0\}, \mathbf{Y} = [L^2(\Omega)]^2,$$

$$M = L_0^2(\Omega) = \left\{ q \in L^2(\Omega) : \int_\Omega q \, dx = 0 \right\},$$

where $\mathbf{V}$ is equipped with the norm $\|\nabla\cdot\|_0$. The scalar product and norm in M are denoted by the usual $L^2(\Omega)$ inner product and its norm $\|\cdot\|_0$, respectively. Spaces consisting of vector-valued functions are denoted in boldface, and the symbol C independent of mesh parameters denotes a generic positive constant whose value may change in different locations. Now, we define the following bilinear and trilinear forms:

$$\begin{cases} a(\mathbf{u},\mathbf{v}) = \nu(\nabla\mathbf{u},\nabla\mathbf{v}),\ d(\mathbf{v},p) = (\operatorname{div}\mathbf{v},p) \quad \forall\mathbf{u},\mathbf{v}\in\mathbf{V}, p\in M, \\ b(\mathbf{u};\mathbf{v},\mathbf{w}) = ((\mathbf{u}\cdot\nabla)\mathbf{v},\mathbf{w}) \quad \forall\mathbf{u},\mathbf{v},\mathbf{w}\in\mathbf{V}. \end{cases}$$

Moreover, if $\operatorname{div}\mathbf{u}=0$, then the trilinear form $b(\cdot;\cdot,\cdot)$ satisfies

$$b(\mathbf{u};\mathbf{v},\mathbf{w}) = ((\mathbf{u}\cdot\nabla)\mathbf{v},\mathbf{w}) + \frac{1}{2}((\operatorname{div}\mathbf{u})\mathbf{v},\mathbf{w}) = \frac{1}{2}((\mathbf{u}\cdot\nabla)\mathbf{v},\mathbf{w}) - \frac{1}{2}((\mathbf{u}\cdot\nabla)\mathbf{w},\mathbf{v}),$$

$$b(\mathbf{u};\mathbf{v},\mathbf{w}) = -b(\mathbf{u};\mathbf{w},\mathbf{v}) \quad \forall\mathbf{u},\mathbf{v},\mathbf{w}\in\mathbf{V}.$$

The following inequality will be used repeatedly in the sequel [21, 22]:

$$|b(\mathbf{u};\mathbf{v},\mathbf{w})| \le N\|\nabla\mathbf{u}\|_0\|\nabla\mathbf{v}\|_0\|\nabla\mathbf{w}\|_0,$$

where

$$N = \sup_{\mathbf{u},\mathbf{v},\mathbf{w}\in\mathbf{V}} \frac{b(\mathbf{u};\mathbf{v},\mathbf{w})}{\|\nabla\mathbf{u}\|_0\|\nabla\mathbf{v}\|_0\|\nabla\mathbf{w}\|_0}.$$

The velocity–pressure variational inequality problem of the second kind for (1.1) and (1.2) is proposed as follows [2]:

Problem VI. Find $(\mathbf{u},p)\in(\mathbf{V},M)$ such that

$$a(\mathbf{u},\mathbf{v}-\mathbf{u}) + b(\mathbf{u};\mathbf{u},\mathbf{v}-\mathbf{u}) - d(\mathbf{v}-\mathbf{u},p) + j(v_\tau) - j(u_\tau) \ge (\mathbf{f},\mathbf{v}-\mathbf{u}) \quad \forall\mathbf{v}\in\mathbf{V}, \tag{2.1a}$$

$$d(\mathbf{u},q) = 0 \quad \forall q\in M, \tag{2.1b}$$

where $j(\eta)$ is the barrier term against slip on Γ_S: $j(\eta)=\int_S g|\eta|ds, \eta\in L^2(\Gamma_S)$. Obviously, j is a continuous functional defined on $L^2(\Gamma_S)$. Considering the selection of the velocity space, another formulation is shown as:

Problem VI$_\sigma$. Find $\mathbf{u}\in\mathbf{V}_\sigma$ such that

$$a(\mathbf{u},\mathbf{v}-\mathbf{u}) + b(\mathbf{u};\mathbf{u},\mathbf{v}-\mathbf{u}) + j(v_\tau) - j(u_\tau) \ge (\mathbf{f},\mathbf{v}-\mathbf{u}) \quad \forall\mathbf{v}\in\mathbf{V}_\sigma. \tag{2.2}$$

Introduce the Lagrange multiplier $\lambda := -\sigma_\tau/g$; then **Problems VI** can be proved to be equivalent to the following variational problem [23]:

Problem VE. Find $(\mathbf{u},p,\lambda)\in(\mathbf{V},M,\tilde{\Lambda})$ such that

$$a(\mathbf{u},\mathbf{v}) + b(\mathbf{u};\mathbf{u},\mathbf{v}) - d(\mathbf{v},p) + (v_\tau,\lambda)_\Lambda = (\mathbf{f},\mathbf{v}) \quad \forall\mathbf{v}\in\mathbf{V}, \tag{2.3a}$$

$$d(\mathbf{u},q) = 0 \quad \forall q\in M, \tag{2.3b}$$

$$(u_\tau,\mu-\lambda)_\Lambda \le 0 \quad \forall\mu\in\tilde{\Lambda}, \tag{2.3c}$$

where Λ is a Hilbert space with its closed convex subset $\tilde{\Lambda}$ defined by

$$\Lambda = L^2(\Gamma_S), \quad (\cdot,\cdot)_\Lambda = (g\cdot,\cdot)_{L^2(\Gamma_S)}, \quad \tilde{\Lambda} = \{\lambda\in\Lambda\,|\,|\lambda|\le 1 \text{ a.e. on } \Gamma_S\},$$

and g is supposed to belong to $L^\infty(\Gamma_S)$. With this λ, the slip boundary conditions can be expressed as

$$|\lambda| < 1 \Rightarrow u_\tau = 0, \quad u_\tau > 0 \Rightarrow \lambda = 1, \quad u_\tau < 0 \Rightarrow \lambda = -1,$$

which we call the slip/no-slip detecting condition.

Existence and uniqueness of a solution to problem (2.2) is given as follows:

Lemma 1 ([4]). *If $\mathbf{f} \in \mathbf{Y}$, $g \in L^2(\Gamma_S)$, and the following condition holds:*

$$\frac{4\kappa N(\|\mathbf{f}\|_0 + \|g\|_{0,\Gamma_S})}{\nu^2} < 1,$$

where $\kappa > 0$ satisfies

$$|(\mathbf{f}, \mathbf{v}) - j(v_\tau)| \le \kappa(\|\mathbf{f}\|_0 + \|g\|_{0,\Gamma_S})\|\nabla \mathbf{v}\|_0 \quad \forall \mathbf{v} \in \mathbf{V}_\sigma,$$

then problem (2.2) admits a unique solution $\mathbf{u}$ *such that*

$$\|\nabla \mathbf{u}\|_0 \le \frac{2\kappa}{\nu}(\|\mathbf{f}\|_0 + \|g\|_{0,\Gamma_S}) \quad \forall \mathbf{u} \in \mathbf{V}_\sigma.$$

III. FINITE ELEMENT APPROXIMATION FOR THE SLIP BOUNDARY CONDITION

A. Triangulation and Approximate Function Spaces

Let $\tau_h = \{K\}$ be a family of shape-regular and conforming triangulations of Ω with $h = \max\{h_K | K \in \tau_h\}, h_K = \mathrm{diam} K, \overline{\Omega} = \cup_K \bar{K}$, and $\partial K_i \cap \partial K_j = e\,(i \ne j)$, where e is a whole edge in τ_h. Let $e' = \partial K \cap \overline{\Gamma}_S$. To construct a Galerkin approximation for (2.1), we consider the following finite element subspaces of $\mathbf{V}$ and M:

$$\mathbf{V}_h \triangleq \mathbf{P}_1 = \left\{ \mathbf{v} \in \mathbf{V} \cap [C^0(\Omega)]^2 : \mathbf{v}|_K \in [P_1(K)]^2 \quad \forall K \in \tau_h \right\},$$

$$M_h \triangleq \begin{cases} P_0 = \{q \in M : q|_K \in P_0(K) \ \ \forall K \in \tau_h\}, \\ P_1 = \{q \in M : q|_K \in P_1(K) \ \ \forall K \in \tau_h\}, \end{cases}$$

where $P_r(K)(r = 0, 1)$ denotes the space of polynomials of degree at most r.

For the finite element spaces $\mathbf{V}_h \times M_h$, the following approximate properties hold: $\forall (\mathbf{v}, q) \in (\mathbf{H}^2(\Omega) \cap \mathbf{V}, H^1(\Omega))$, there exist approximations $\mathscr{L}_h \mathbf{v} \in \mathbf{V}_h$ and $\mathscr{I}_h q \in M_h$:

$$\|\mathbf{v} - \mathscr{L}_h \mathbf{v}\|_0 + h(\|\nabla(\mathbf{v} - \mathscr{L}_h \mathbf{v})\|_0 + \|q - \mathscr{I}_h q\|_0) \le Ch^2 \|\mathbf{v}\|_2, \tag{3.1}$$

where $\mathscr{L}_h, \mathscr{I}_h$ are two Lagrange interpolation operators.

As is known, the lowest equal-order pair $\mathbf{P}_1 - P_1$ and the conforming pair $\mathbf{P}_1 - P_0$ are unstable because they do not satisfy the so-called inf-sup condition [21, 24]. To overcome this issue and derive optimal error estimates for the mixed finite element solution, a local pressure projection stabilization method is recalled [25]. Let $\Pi_h^j (j = 0, 1)$ be the standard projection operator [25, 26], which is defined as follows:

$$\Pi_h^0 : L^2(\Omega) \to P_0 \quad \text{and} \quad \Pi_h^1 : L^2(\Omega) \to P_1.$$

The interpolation error is introduced here and will be used in the theoretical analysis:

$$\|\Pi_h^j p\|_0 \le \|p\|_0 \ \forall p \in L^2(\Omega) \quad \text{and} \quad \|p - \Pi_h^j p\|_0 \le Ch \ \|p\|_1 \ \forall p \in H^1(\Omega) \cap M. \tag{3.2}$$

Now, we introduce the stabilization bilinear form $G(p, q)$ by the following manner:

$$G(p, q) = (p - \Pi_h^j p, q - \Pi_h^j q) \quad p, q \in M_h.$$

For approximate functions defined on the boundary Γ_S, we define

$$\Lambda_h = \left\{\mu_h \in C^0(\overline{\Gamma}_S) |\ \mu_h|_{e'} \in P_1(e'),\ \mu_h(Q_1) = \mu_h(Q_{m+1}), \{Q_1, Q_{m+1}\} = \overline{\Gamma}_D \cap \overline{\Gamma}_S\right\},$$

$$\tilde{\Lambda}_h = \{\mu_h \in \Lambda_h |\ |\mu_h| \le 1\}.$$

The space Λ_h becomes a Hilbert space if its inner product is given as

$$(\lambda_h, \mu_h)_{\Lambda_h} = \frac{1}{6} \sum_i |e_i| (g_i \lambda_{h,i} \mu_{h,i} + 4 g_{i+\frac{1}{2}} \lambda_{h,i+\frac{1}{2}} \mu_{h,i+\frac{1}{2}} + g_{i+1} \lambda_{h,i+1} \mu_{h,i+1})\ \lambda_h, \mu_h \in \Lambda_h,$$

which approximates $\int_{\Gamma_S} g \lambda_h \mu_h$ by Simpson's formula and $g_i = g(Q_i)$. Q_i and $Q_{i+\frac{1}{2}}$ represent the vertices of the triangles in τ_h and the midpoint of Q_i and Q_{i+1}, $e_i = [Q_i, Q_{i+1}]$ with its length by $|e_i| = |Q_i Q_{i+1}|$ for all $i = 1, 2, \ldots, \mathcal{N}$, and $\mathcal{N}$ is the total number of vertices of the subdivisional triangles.

Finally, to approximate j given in (2.1a), we introduce j_h as

$$j_h(\eta_h) = \frac{1}{6} \sum_i |e_i| (g_i |\eta_{h,i}| + 4 g_{i+\frac{1}{2}} |\eta_{h,i+\frac{1}{2}}| + g_{i+1} |\eta_{h,i+1}|) \quad \eta_h \in \Lambda_h,$$

again with Simpson's formula. Clearly, j_h is a positive continuous and positively homogeneous functional defined on Λ_h. This definition of j_h is motivated by Glowinski [27].

Lemma 2 ([6]). *If $g \in C^2(\overline{\Gamma}_S)$ and $\eta_h \in \Lambda_h$ keeps its sign unchanged on every side, then*

$$|j_h(\eta_h) - j(\eta_h)| \le Ch^2 ||\eta_h||_{0,\Gamma_S}.$$

Remark. An element $\eta_h \in \Lambda_h$ is said to keep a constant sign on every side if for any $i = 1, 2, \ldots, N$, either of the two conditions is satisfied: $\eta_h|_{e_i} \ge 0$ or $\eta_h|_{e_i} \le 0$.

B. Finite Element Discretization

In the following part, we propose the finite element approximation to (2.1) and (2.3):

Problem VI$_h$. Find $(\mathbf{u}_h, p_h) \in (\mathbf{V}_h, M_h)$ such that

$$a(\mathbf{u}_h, \mathbf{v}_h - \mathbf{u}_h) + b(\mathbf{u}_h; \mathbf{u}_h, \mathbf{v}_h - \mathbf{u}_h) - d(\mathbf{v}_h - \mathbf{u}_h, p_h) + j_h(v_{h\tau}) - j_h(u_{h\tau}) \ge (\mathbf{f}, \mathbf{v}_h - \mathbf{u}_h), \tag{3.3a}$$

$$d(\mathbf{u}_h, q_h) + G(p_h, q_h) = 0 \quad \forall \mathbf{v}_h \in \mathbf{V}_h,\ q_h \in M_h. \tag{3.3b}$$

Problem VE$_h$. Find $(\mathbf{u}_h, p_h, \lambda_h) \in (\mathbf{V}_h, M_h, \tilde{\Lambda}_h)$ such that

$$a(\mathbf{u}_h, \mathbf{v}_h) + b(\mathbf{u}_h; \mathbf{u}_h, \mathbf{v}_h) - d(\mathbf{v}_h, p_h) + (v_{h\tau}, \lambda_h) = (\mathbf{f}, \mathbf{v}_h), \tag{3.4a}$$

$$d(\mathbf{u}_h, q_h) + G(p_h, q_h) = 0 \quad \forall \mathbf{v}_h \in \mathbf{V}_h,\ q_h \in M_h. \tag{3.4b}$$

$$(u_{h\tau}, \mu_h - \lambda_h)_{\Lambda_h} \le 0 \quad \forall \mu_h \in \tilde{\Lambda}_h. \tag{3.4c}$$

Let $\mathcal{B}((\mathbf{u}, p); (\mathbf{v}, q)) = a(\mathbf{u}, \mathbf{v}) - d(\mathbf{v}, p) + d(\mathbf{u}, q)$, $\mathcal{B}_h((\mathbf{u}_h, p_h); (\mathbf{v}_h, q_h)) = \mathcal{B}((\mathbf{u}_h, p_h); (\mathbf{v}_h, q_h)) + G(p_h, q_h)$; the stability of $\mathcal{B}_h((\cdot,\cdot);(\cdot,\cdot))$, existence and uniqueness of a solution to the discrete **Problem VI**$_h$ are stated as follows:

Lemma 3 ([4, 26]). *For all* $(\mathbf{u}_h, p_h) \in (\mathbf{V}_h, M_h)$*, there exist two positive constants* β_1 *and* β_2*, independent of h, such that*

$$|\mathcal{B}_h((\mathbf{u}_h, p_h); (\mathbf{v}_h, q_h))| \le \beta_1(\|\nabla \mathbf{u}_h\|_0 + \|p_h\|_0)(\|\nabla \mathbf{v}_h\|_0 + \|q_h\|_0),$$

$$\beta_2(\|\nabla \mathbf{u}_h\|_0 + \|p_h\|_0) \le \sup_{0 \ne (\mathbf{v}_h, q_h) \in (\overset{\circ}{\mathbf{V}}_h, M_h)} \frac{\mathcal{B}_h((\mathbf{u}_h, p_h); (\mathbf{v}_h, q_h))}{\|\nabla \mathbf{v}_h\|_0 + \|q_h\|_0},$$

where $\overset{\circ}{\mathbf{V}}_h = \mathbf{V}_h \cap \mathbf{H}_0^1(\Omega)$.

Lemma 4 ([4]). *Under the conditions of Lemmas 1 and 3, the discrete problem (3.3) admits a unique solution* $(\mathbf{u}_h, p_h)$ *satisfying*

$$\|\nabla \mathbf{u}_h\|_0 \le \frac{2\kappa}{\nu}(\|\mathbf{f}\|_0 + \|g\|_{0,\Gamma_S}), \quad \|p_h\|_0 \le \frac{\|\mathbf{f}\|_0 + \kappa(\|\mathbf{f}\|_0 + \|g\|_{0,\Gamma_S})}{\beta_2}.$$

Theorem 5. *Corresponding to the continuous variation, the discrete* ***Problem VI***$_h$ *and* ***Problem VE***$_h$ *are equivalent.*

Proof. Let $(\mathbf{u}_h, p_h) \in (\mathbf{V}_h, M_h)$ be a solution of **Problem VI**$_h$. Taking $\mathbf{u}_h \pm \mathbf{v}_h$ as a test function in (3.3a) with an arbitrary $\mathbf{v}_h \in \overset{\circ}{\mathbf{V}}_h$, yields

$$a(\mathbf{u}_h, \mathbf{v}_h) + b(\mathbf{u}_h; \mathbf{u}_h, \mathbf{v}_h) - d(\mathbf{v}_h, p_h) = (\mathbf{f}, \mathbf{v}_h).$$

As $\left\{\mathbf{v}_h \in \mathbf{V}_h \mid (v_{h\tau}, \eta_h)_{\Lambda_h} = 0, \forall \eta_h \in \Lambda_h\right\} = \overset{\circ}{\mathbf{V}}_h$, it satisfies the inf-sup condition in [6]

$$\beta_h ||\eta_h||_{\Lambda_h} \le \sup_{\mathbf{v}_h \in \mathbf{V}_h} \frac{(v_{h\tau}, \eta_h)_{\Lambda_h}}{||\nabla \mathbf{v}_h||_0} \quad \forall \eta_h \in \Lambda_h,$$

where $||\cdot||_{\Lambda_h}$ is defined by the inner product in space Λ_h. Then, there exists a unique $\lambda_h \in \Lambda_h$ such that (3.4a) holds. Choosing $\mathbf{v}_h = \mathbf{v}_h - \mathbf{u}_h$ in (3.4a) and subtracting with (3.3a) gives

$$(v_{h\tau} - u_{h\tau}, \lambda_h)_{\Lambda_h} \le j_h(v_{h\tau}) - j_h(u_{h\tau}) \le j_h(v_{h\tau} - u_{h\tau}) \quad \forall \mathbf{v}_h \in \mathbf{V}_h, \tag{3.5}$$

so that $(\eta_h, \lambda_h)_{\Lambda_h} \le j_h(\eta_h)$, $\forall \eta_h \in \Lambda_h$, which is equivalent to $\lambda_h \in \tilde{\Lambda}_h$. Finally, we prove (3.4c). Taking $\mathbf{v}_h = 0$ in (3.5), we have $j_h(u_{h\tau}) \le (u_{h\tau}, \lambda_h)_{\Lambda_h}$. Because $j_h(u_{h\tau}) \le (u_{h\tau}, \lambda_h)_{\Lambda_h} \Leftrightarrow (u_{h\tau}, \mu_h - \lambda_h)_{\Lambda_h} \le 0$, $\forall \mu_h \in \tilde{\Lambda}_h$, this implies (3.4c). Therefore, $(\mathbf{u}_h, p_h, \lambda_h)$ solves **Problem VE**$_h$.

Conversely, if $(\mathbf{u}_h, p_h, \lambda_h) \in (\mathbf{V}_h, M_h, \tilde{\Lambda}_h)$ is a solution of **Problem VE**$_h$. It follows from (3.4c) that $(u_{h\tau}, \lambda_h)_{\Lambda_h} = j_h(u_{h\tau})$, in addition, as $v_{h\tau} \in \mathbf{V}_h, \lambda_h \in \tilde{\Lambda}_h$, which can detrude that $(v_{h\tau}, \lambda_h)_{\Lambda_h} \le j_h(v_{h\tau})$, then we have

$$(v_{h\tau} - u_{h\tau}, \lambda_h)_{\Lambda_h} = (v_{h\tau}, \lambda_h)_{\Lambda_h} - (u_{h\tau}, \lambda_h)_{\Lambda_h} \le j_h(v_{h\tau}) - j_h(u_{h\tau}).$$

Choosing $\mathbf{v}_h = \mathbf{v}_h - \mathbf{u}_h$ in (3.4a) and combining with the above formula can obtain (3.3a).

For more details of the proof about this theorem, such as the proof of the inf-sup condition and the equivalence relation which we omit here, the reader could find in the recent work by Kashiwabara [6] (Lemma 3.1–3.3) and [7]. ∎

IV. OPTIMAL ANALYSIS

In this section, we analyze the error estimates of the stabilized finite element methods for the blood flow model of arteriosclerosis governed by (1.1) and (1.2). To get the optimal order of convergence, some additional assumptions are made for the next theorem: $(\mathscr{L}_\Lambda \mathbf{u})_\tau$ and $u_{h\tau}$ have the constant sign on every side and $\mathrm{sgn}(u_\tau) = \mathrm{sgn}((\mathscr{L}_h \mathbf{u})_\tau)$ on Γ_S.

Theorem 6. *Under the conditions of Lemmas 1, 2, 3, and 4, we assume $g \in C^2(\overline{\Gamma}_S) \cap L^2(\Gamma_S)$, let $(\mathbf{u}, p) \in (\mathbf{V}, M)$ and $(\mathbf{u}_h, p_h) \in (\mathbf{V_h}, M_h)$ be the solutions of (2.1) and (3.3), respectively. Then the following error estimate holds:*

$$\|\nabla(\mathbf{u} - \mathbf{u}_h)\|_0 + \|p - p_h\|_0 \le Ch, \tag{4.1}$$

where $C > 0$ is dependent of $(\nu, \mathbf{f}, g, \Omega)$.

Proof. For all $\mathbf{v}_h \in \mathbf{V}_h$ and $q_h \in M_h$, it is obvious that

$$a(\mathbf{u} - \mathbf{u}_h, \mathbf{u} - \mathbf{u}_h) = a(\mathbf{u} - \mathbf{u}_h, \mathbf{u} - \mathbf{v}_h) - a(\mathbf{u}, \mathbf{u}_h - \mathbf{u}) - a(\mathbf{u}_h, \mathbf{v}_h - \mathbf{u}_h) + a(\mathbf{u}, \mathbf{v}_h - \mathbf{u}).$$

Substitute (2.1a) with $\mathbf{v} = \mathbf{u}_h$, (3.3a) with $\mathbf{v}_h$ itself and (2.3a) with $\mathbf{v} = \mathbf{v}_h - \mathbf{u}$ into the second, third, and fourth terms of the right-hand side in the above equation, respectively. Combining with Korn's inequality, we deduce

$$\begin{aligned}
\nu||\nabla(\mathbf{u} - \mathbf{u}_h)||_0^2 &\le a(\mathbf{u} - \mathbf{u}_h, \mathbf{u} - \mathbf{v}_h) \\
&\quad + b(\mathbf{u}; \mathbf{u}, \mathbf{u}_h - \mathbf{u}) - d(\mathbf{u}_h - \mathbf{u}, p) + j(u_{h\tau}) - j(u_\tau) - (\mathbf{f}, \mathbf{u}_h - \mathbf{u}) \\
&\quad + b(\mathbf{u}_h; \mathbf{u}_h, \mathbf{v}_h - \mathbf{u}_h) - d(\mathbf{v}_h - \mathbf{u}_h, p_h) + j_h(v_{h\tau}) - j_h(u_{h\tau}) - (\mathbf{f}, \mathbf{v}_h - \mathbf{u}_h) \\
&\quad - b(\mathbf{u}; \mathbf{u}, \mathbf{v}_h - \mathbf{u}) + d(\mathbf{v}_h - \mathbf{u}, p) - (v_{h\tau} - u_\tau, \lambda)_\Lambda + (\mathbf{f}, \mathbf{v}_h - \mathbf{u}) \\
&\le a(\mathbf{u} - \mathbf{u}_h, \mathbf{u} - \mathbf{v}_h) + b(\mathbf{u} - \mathbf{u}_h; \mathbf{u}, \mathbf{u}_h - \mathbf{u}) + b(\mathbf{u}_h; \mathbf{u} - \mathbf{u}_h, \mathbf{u}_h - \mathbf{u}) \\
&\quad + b(\mathbf{u}_h; \mathbf{u}_h - \mathbf{u}, \mathbf{v}_h - \mathbf{u}) + b(\mathbf{u}_h - \mathbf{u}; \mathbf{u}, \mathbf{v}_h - \mathbf{u}) - d(\mathbf{u}_h - \mathbf{u}, p - q_h) \\
&\quad - d(\mathbf{v}_h - \mathbf{u}, p_h - p) + G(p_h, p_h - q_h) + j(u_{h\tau}) - j(u_\tau) + j_h(v_{h\tau}) \\
&\quad - j_h(u_{h\tau}) - (v_{h\tau} - u_\tau, \lambda)_\Lambda.
\end{aligned} \tag{4.2}$$

As $\sigma_\tau u_\tau + g|u_\tau| = 0, \sigma_\tau = -g\lambda$, from [6], we know that $(v_{h\tau} - u_\tau, \lambda)_\Lambda + j(v_{h\tau}) - j(u_\tau) = 0$. Setting $\mathbf{v}_h = \mathscr{L}_h\mathbf{u}$, $q_h = \Pi_h^j p$, (4.2) turns into

$$\begin{aligned}\nu||\nabla(\mathbf{u}-\mathbf{u}_h)||_0^2 &\le a(\mathbf{u}-\mathbf{u}_h, \mathbf{u}-\mathscr{L}_h\mathbf{u}) + b(\mathbf{u}-\mathbf{u}_h; \mathbf{u}, \mathbf{u}_h-\mathbf{u}) + b(\mathbf{u}_h; \mathbf{u}-\mathbf{u}_h, \mathbf{u}_h-\mathbf{u})\\ &+ b(\mathbf{u}_h; \mathbf{u}_h-\mathbf{u}, \mathscr{L}_h\mathbf{u}-\mathbf{u}) + b(\mathbf{u}_h-\mathbf{u}; \mathbf{u}, \mathscr{L}_h\mathbf{u}-\mathbf{u}) - d(\mathbf{u}_h-\mathbf{u}, p-\Pi_h^j p)\\ &- d(\mathscr{L}_h\mathbf{u}-\mathbf{u}, p_h-p) + G(p_h, p_h-\Pi_h^j p) + j(u_{h\tau}) + j_h((\mathscr{L}_h\mathbf{u})_\tau) - j_h(u_{h\tau}) - j((\mathscr{L}_h\mathbf{u})_\tau).\end{aligned} \tag{4.3}$$

Next, using (3.1) and (3.2), we give the estimates for each term of the right-hand side in (4.3):

$$\begin{aligned}&|a(\mathbf{u}-\mathbf{u}_h, \mathbf{u}-\mathscr{L}_h\mathbf{u})| \le Ch||\nabla(\mathbf{u}-\mathbf{u}_h)||_0,\\ &|b(\mathbf{u}-\mathbf{u}_h; \mathbf{u}, \mathbf{u}_h-\mathbf{u}) + b(\mathbf{u}_h; \mathbf{u}-\mathbf{u}_h, \mathbf{u}_h-\mathbf{u})|\\ &\quad\le N(||\nabla\mathbf{u}||_0 + ||\nabla\mathbf{u}_h||_0)||\nabla(\mathbf{u}-\mathbf{u}_h)||_0^2 \le C||\nabla(\mathbf{u}-\mathbf{u}_h)||_0^2,\\ &|b(\mathbf{u}_h; \mathbf{u}_h-\mathbf{u}, \mathscr{L}_h\mathbf{u}-\mathbf{u}) + b(\mathbf{u}_h-\mathbf{u}; \mathbf{u}, \mathscr{L}_h\mathbf{u}-\mathbf{u})|\\ &\quad\le N(||\nabla\mathbf{u}||_0 + ||\nabla\mathbf{u}_h||_0)||\nabla(\mathbf{u}-\mathbf{u}_h)||_0||\nabla(\mathbf{u}-\mathscr{L}_h\mathbf{u})||_0 \le Ch||\nabla(\mathbf{u}-\mathbf{u}_h)||_0,\\ &|d(\mathbf{u}_h-\mathbf{u}, p-\Pi_h^j p)| \le C||\nabla(\mathbf{u}-\mathbf{u}_h)||_0||p-\Pi_h^j p||_0 \le Ch||\nabla(\mathbf{u}-\mathbf{u}_h)||_0,\\ &|-d(\mathscr{L}_h\mathbf{u}-\mathbf{u}, p_h-p)| \le C||\nabla(\mathbf{u}-\mathscr{L}_h\mathbf{u})||_0||p-p_h||_0 \le Ch||p-p_h||_0,\\ &|G(p_h, p_h-\Pi_h^j p)| \le Ch||p_h||_1||p_h-\Pi_h^j p||_0.\end{aligned}$$

By Lemma 2, we see that

$$\begin{aligned}&|j(u_{h\tau}) - j_h(u_{h\tau})| \le Ch^2||u_{h\tau}||_{0,\Gamma_S} \le Ch^2||\nabla\mathbf{u}_h||_0 \le Ch^2.\\ &|j_h((\mathscr{L}_h\mathbf{u})_\tau) - j((\mathscr{L}_h\mathbf{u})_\tau)| \le Ch^2||(\mathscr{L}_h\mathbf{u})_\tau||_{0,\Gamma_S} \le Ch^2||\mathscr{L}_h\mathbf{u}||_1 \le Ch^2.\end{aligned}$$

Combining these estimates with (4.3), we deduce

$$||\nabla(\mathbf{u}-\mathbf{u}_h)||_0^2 \le Ch(||\nabla(\mathbf{u}-\mathbf{u}_h)||_0 + ||p-p_h||_0) + Ch^2. \tag{4.4}$$

In view of the triangle inequality, $||p-p_h||_0 \le ||p-q_h||_0 + ||p_h-q_h||_0$. Then, we estimate $||p_h-q_h||_0$. Taking $\mathbf{u} \pm \mathbf{w}_h$ as a test function in (2.1a), with an arbitrary $\mathbf{w}_h \in \mathring{\mathbf{V}}_h$, yields

$$a(\mathbf{u}, \mathbf{w}_h) + b(\mathbf{u}; \mathbf{u}, \mathbf{w}_h) - d(\mathbf{w}_h, p) = (\mathbf{f}, \mathbf{w}_h).$$

Conversely, we can similarly show that

$$a(\mathbf{u}_h, \mathbf{w}_h) + b(\mathbf{u}_h; \mathbf{u}_h, \mathbf{w}_h) - d(\mathbf{w}_h, p_h) = (\mathbf{f}, \mathbf{w}_h) \quad \forall\mathbf{w}_h \in \mathring{\mathbf{V}}_h\ .$$

By subtraction, we obtain

$$a(\mathbf{u}-\mathbf{u}_h, \mathbf{w}_h) + b(\mathbf{u}; \mathbf{u}, \mathbf{w}_h) - b(\mathbf{u}_h; \mathbf{u}_h, \mathbf{w}_h) - d(\mathbf{w}_h, p-p_h) = 0 \quad \forall\mathbf{w}_h \in \mathring{\mathbf{V}}_h\ .$$

According to Lemma 3, we have

$$\beta_2||p_h-q_h||_0 \le \sup_{(\mathbf{w}_h, q_h)\in(\mathring{\mathbf{V}}_h, M_h)} \frac{\mathcal{B}_h((\mathbf{u}_h-\mathbf{v}_h, p_h-q_h); (\mathbf{w}_h, q_h))}{||\nabla\mathbf{w}_h||_0 + ||q_h||_0}$$

$$\leq \sup_{(\mathbf{w}_h,q_h)\in(\overset{\circ}{\mathbf{V}}_h,M_h)} \frac{\mathcal{B}_h((\mathbf{u}_h-\mathbf{u},p_h-p);(\mathbf{w}_h,q_h))+\mathcal{B}_h((\mathbf{u}-\mathbf{v}_h,p-q_h);(\mathbf{w}_h,q_h))}{||\nabla\mathbf{w}_h||_0+||q_h||_0}$$

$$\leq \sup_{(\mathbf{w}_h,q_h)\in(\overset{\circ}{\mathbf{V}}_h,M_h)} \frac{b(\mathbf{u}_h;\mathbf{u}_h,\mathbf{w}_h)-b(\mathbf{u};\mathbf{u},\mathbf{w}_h)-G(p,q_h)+\mathcal{B}_h((\mathbf{u}-\mathbf{v}_h,p-q_h);(\mathbf{w}_h,q_h))}{||\nabla\mathbf{w}_h||_0+||q_h||_0}$$

$$\leq C(||\nabla(\mathbf{u}-\mathbf{u}_h)||_0+||p-q_h||_0+||\nabla(\mathbf{u}-\mathbf{v}_h)||_0+||p-q_h||_0). \tag{4.5}$$

Also considering that $\mathbf{v}_h=\mathscr{L}_h\mathbf{u}, q_h=\Pi_h^j p$, according to (3.1), (3.2) and combining (4.4), (4.5), this proof is completed. ∎

Next, we estimate the error $\|\mathbf{u}-\mathbf{u}_h\|_0$ using the parabolic duality argument for a linearized Navier–Stokes problem [21]: Seek $(\boldsymbol{\phi},\psi)\in(\mathbf{V},M)$ such that, for $\mathbf{z}\in\mathbf{Y}$,

$$\begin{cases} a(\boldsymbol{\phi},\mathbf{v})+b(\mathbf{u};\mathbf{v},\boldsymbol{\phi})+b(\mathbf{v};\mathbf{u},\boldsymbol{\phi})-d(\mathbf{v},\psi)=(\mathbf{v},\mathbf{z}),\\ d(\boldsymbol{\phi},q)=0 \quad \forall(\mathbf{v},q)\in(\mathbf{V},M). \end{cases} \tag{4.6}$$

This problem is well posed and has a unique solution $(\boldsymbol{\phi},\psi)\in(\mathbf{H}^2(\Omega)\cap\mathbf{V},H^1(\Omega)\cap M)$ satisfying

$$\|\boldsymbol{\phi}\|_2+\|\psi\|_1\leq C\|\mathbf{z}\|_0. \tag{4.7}$$

Let $(\boldsymbol{\phi}_h,\psi_h)\in(\overset{\circ}{\mathbf{V}}_h,M_h)$ be the stabilized finite element approximation solution of (4.6). Then, there exists a positive constant C with the following error estimate:

$$\|\nabla(\boldsymbol{\phi}-\boldsymbol{\phi}_h)\|_0+\|\psi-\psi_h\|_0\leq Ch\|\mathbf{z}\|_0. \tag{4.8}$$

Theorem 7. *Under the conditions of Lemmas 1, 3 and 4, let* $(\mathbf{u},p)\in(\mathbf{V},M)$ *and* $(\mathbf{u}_h,p_h)\in(\mathbf{V}_h,M_h)$ *be the solutions of (2.1) and (3.3), respectively. Then there exists a constant* $C>0$ *independent of h, the following error estimate holds:*

$$\|\mathbf{u}-\mathbf{u}_h\|_0\leq Ch^2.$$

Proof. Let $\mathbf{e}=\mathbf{u}-\mathbf{u}_h$. For $\boldsymbol{\phi}_h\in\overset{\circ}{\mathbf{V}}_h$, taking $\mathbf{v}=\mathbf{u}\pm\boldsymbol{\phi}_h\in\mathbf{V}$ in (2.1a) and $\mathbf{v}_h=\mathbf{u}_h\pm\boldsymbol{\phi}_h\in\mathbf{V}_h$ in (3.3a) and subtracting the resulting equations give

$$a(\mathbf{e},\boldsymbol{\phi}_h)+b(\mathbf{e};\mathbf{u},\boldsymbol{\phi}_h)+b(\mathbf{u}_h;\mathbf{e},\boldsymbol{\phi}_h)-d(\boldsymbol{\phi}_h,p-p_h)=0.$$

Adding the above equation to $d(\boldsymbol{\phi},q)=0, q\in M$ yields

$$a(\mathbf{e},\boldsymbol{\phi}_h)+b(\mathbf{e};\mathbf{u},\boldsymbol{\phi}_h)+b(\mathbf{u}_h;\mathbf{e},\boldsymbol{\phi}_h)+d(\boldsymbol{\phi}-\boldsymbol{\phi}_h,p-p_h)=0. \tag{4.9}$$

Next, setting $(\mathbf{v},q)=(\mathbf{e},\psi)$ and $\mathbf{z}=\mathbf{e}$ in (4.6), it holds that

$$\|\mathbf{e}\|_0^2=a(\boldsymbol{\phi},\mathbf{e})+b(\mathbf{u};\mathbf{e},\boldsymbol{\phi})+b(\mathbf{e};\mathbf{u},\boldsymbol{\phi})-d(\mathbf{e},\boldsymbol{\phi}). \tag{4.10}$$

Substituting (4.9) into (4.10), we have

$$\begin{aligned}\|\mathbf{e}\|_0^2=&\,a(\boldsymbol{\phi}-\boldsymbol{\phi}_h,\mathbf{e})+b(\mathbf{u}_h;\mathbf{e},\boldsymbol{\phi}-\boldsymbol{\phi}_h)+b(\mathbf{e};\mathbf{u},\boldsymbol{\phi}-\boldsymbol{\phi}_h)+b(\mathbf{e};\mathbf{e},\boldsymbol{\phi})\\&-d(\mathbf{e},\psi)-d(\boldsymbol{\phi}-\boldsymbol{\phi}_h,p-p_h).\end{aligned} \tag{4.11}$$

Letting $q = q_h$ in (2.1b) and combining (3.3b) with it, we see that

$$d(\mathbf{e}, q_h) - G(p_h, q_h) = 0 \quad \forall q_h \in M_h.$$

In the above equation, we choose $q_h = \psi_h$ to have

$$d(\mathbf{e}, \psi) = d(\mathbf{e}, \psi - \psi_h) - G(p_h, \psi_h).$$

Then, Eq. (4.11) turns into

$$\begin{aligned}
\|\mathbf{e}\|_0^2 &= a(\boldsymbol{\phi} - \boldsymbol{\phi}_h, \mathbf{e}) + b(\mathbf{u}; \mathbf{e}, \boldsymbol{\phi} - \boldsymbol{\phi}_h) + b(\mathbf{e}; \mathbf{u}, \boldsymbol{\phi} - \boldsymbol{\phi}_h) + b(\mathbf{e}; \mathbf{e}, \boldsymbol{\phi}_h) - d(\mathbf{e}, \psi - \psi_h) \\
&\quad - d(\boldsymbol{\phi} - \boldsymbol{\phi}_h, p - p_h) + G(p_h, \psi_h) \\
&\le \nu \|\nabla(\boldsymbol{\phi} - \boldsymbol{\phi}_h)\|_0 \|\nabla \mathbf{e}\|_0 + N(\|\nabla \mathbf{u}\|_0 + \|\nabla \mathbf{u}_h\|_0)\|\nabla \mathbf{e}\|_0 \|\nabla(\boldsymbol{\phi} - \boldsymbol{\phi}_h)\|_0 \\
&\quad + C\|\nabla \mathbf{e}\|_0^2 \|\boldsymbol{\phi}\|_2 + C\|\nabla \mathbf{e}\|_0 \|\psi - \psi_h\|_0 + C\|\nabla(\boldsymbol{\phi} - \boldsymbol{\phi}_h)\|_0 \|p - p_h\|_0 \\
&\quad + Ch\|\psi - \psi_h\|_0 + Ch^2\|\psi\|_1 \\
&\le Ch(\|\nabla \mathbf{e}\|_0 + \|p - p_h\|_0)\|\mathbf{e}\|_0 + Ch^2\|\mathbf{e}\|_0.
\end{aligned}$$

Due to

$$\begin{aligned}
|G(p_h, \psi_h)| &= |-G(p_h - \Pi_h^j p_h, \psi - \psi_h) + G(p_h - \Pi_h^j p_h, \psi - \Pi_h^j \psi)| \\
&\le Ch\|p_h\|_1 \|\psi - \psi_h\|_0 + Ch^2 \|p_h\|_1 \|\psi\|_1,
\end{aligned}$$

together with Eqs. (4.1, 4.7), and (4.8), we obtain

$$\|\mathbf{u} - \mathbf{u}_h\|_0 \le Ch^2,$$

which completes the proof. ∎

V. NUMERICAL EXAMPLES

In this section, we present some numerical tests to check the theoretical analysis obtained in Section IV. We apply the following Uzawa iterative algorithm introduced in [6] to solve the discrete variational inequality problem numerically: Choosing an arbitrary λ_h^1,

Step 1. Give $\lambda_h^1 \in \tilde{\Lambda}_h$ and $\rho > 0$, $n := 1$,
Step 2. With λ_h^n known, seek $(\mathbf{u}_h^n, p_h^n)$ satisfying

$$\begin{cases} a(\mathbf{u}_h^n, \mathbf{v}_h) + b(\mathbf{u}_h^n; \mathbf{u}_h^n, \mathbf{v}_h) - d(\mathbf{v}_h, p_h^n) = (\mathbf{f}, \mathbf{v}_h) - (v_{h\boldsymbol{\tau}}, \lambda_h^n)_{\Lambda_h} & \forall \mathbf{v}_h \in \mathbf{V}_h, \\ d(\mathbf{u}_h^n, q_h) + G(p_h^n, q_h) = 0 & \forall q_h \in M_h, \end{cases}$$

Step 3. Set $n := n + 1$ and renew λ_h^{n+1} with $\lambda_h^{n+1} = P_{\tilde{\Lambda}_h}(\lambda_h^n + \rho u_{h\boldsymbol{\tau}}^n)$.

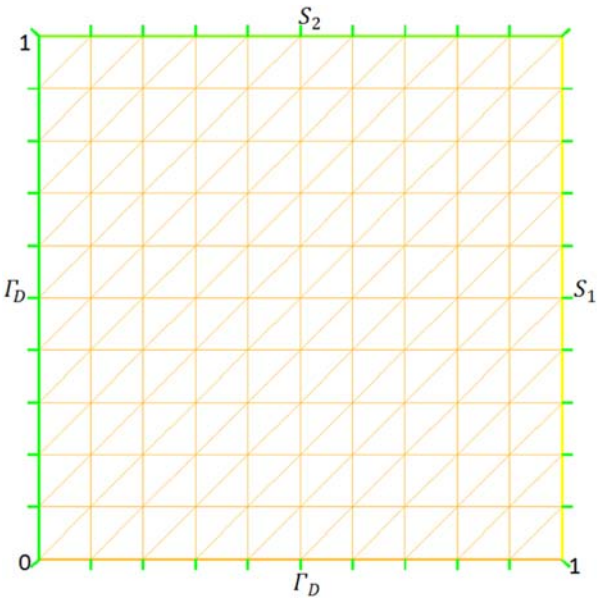

FIG. 1. Mesh of domain Ω with $\Gamma_S = S_1 \cup S_2$ ($h = \frac{1}{10}$). [Color figure can be viewed in the online issue, which is available at wileyonlinelibrary.com.]

If reaching the predefined accuracy or iteration steps, stop computing; otherwise, continue Step 2. The projection operator $P_{\tilde{\Lambda}_h} : \Lambda_h \to \tilde{\Lambda}_h$ is explicitly expressed as

$$P_{\tilde{\Lambda}_h} = \begin{cases} +1 & \text{if } \mu_h(Q) > 1 \\ \mu_h(M) & \text{if } |\mu_h(Q)| \le 1 \\ -1 & \text{if } \mu_h(Q) < -1 \end{cases} \quad (\forall \mu_h(Q) \in \Lambda_h).$$

This projection is equivalent to (3.4c) [6]. In addition, the Newton iteration method [28] is used in Step 2 when calculating the nonlinear term $b(\cdot;\cdot,\cdot)$. Next, we will demonstrate some examples to illustrate our theoretical expectation.

A. Analytical Solution Problem

Let $\Omega = (0,1) \times (0,1)$ (see Fig. 1), $\nu = 1$ and the exact solution $(\mathbf{u}, p)$ of the Navier–Stokes Eq. (1.1) be

$$\mathbf{u}(x,y) = (u_1(x,y), u_2(x,y)), \quad p(x,y) = (2x-1)(2y-1),$$
$$u_1(x,y) = -x^2 y(x-1)(3y-2), \quad u_2(x,y) = xy^2(y-1)(3x-2).$$

Then, the function $\mathbf{f}$ is defined by (1.1), and it is easy to verify that the exact solution $\mathbf{u}$ satisfies the boundary conditions (1.2) on Γ_D and Γ_S. By simple calculations, we state σ_τ directly:

$$\begin{cases} \sigma_\tau = 4\nu y^2(1-y) & \text{on } S_1, \\ \sigma_\tau = 4\nu x^2(1-x) & \text{on } S_2. \end{cases}$$

TABLE I. Error estimates for velocity and pressure under different finite element pairs

	Stabilized $\mathbf{P_1} - P_1$ finite element pair			Stabilized $\mathbf{P_1} - P_0$ finite element pair		
$\frac{1}{h}$	$\frac{\|p-p_h\|_0}{\|p\|_0}$	$\frac{\|\nabla(\mathbf{u}-\mathbf{u}_h)\|_0}{\|\nabla\mathbf{u}\|_0}$	$\frac{\|\mathbf{u}-\mathbf{u}_h\|_0}{\|\mathbf{u}\|_0}$	$\frac{\|p-p_h\|_0}{\|p\|_0}$	$\frac{\|\nabla(\mathbf{u}-\mathbf{u}_h)\|_0}{\|\nabla\mathbf{u}\|_0}$	$\frac{\|\mathbf{u}-\mathbf{u}_h\|_0}{\|\mathbf{u}\|_0}$
10	0.107265	0.231956	0.0530028	0.248186	0.2338	0.0756685
20	0.0366426	0.115771	0.01300376	0.119961	0.115795	0.0191768
30	0.0194626	0.0769543	0.00574208	0.0781955	0.0768829	8.5024 E−3
40	0.0124411	0.0576069	3.21358 E−3	0.0578606	0.0575427	4.77113 E−3
50	8.80354 E−3	0.0460275	2.05016 E−3	0.0458824	0.0459771	3.04807 E−3
60	6.6422 E−3	0.0383221	1.042064E−4	0.0380004	0.0382828	2.11392 E−3

TABLE II. Convergence rates of different finite element pairs

	Stabilized $\mathbf{P}_1 - P_1$ finite element pair			Stabilized $\mathbf{P}_1 - P_0$ finite element pair		
$\frac{1}{h}$	p_{L^2} rate	$\mathbf{u}_{H^1}$ rate	$\mathbf{u}_{L^2}$ rate	p_{L^2} rate	$\mathbf{u}_{H^1}$ rate	$\mathbf{u}_{L^2}$ rate
10	/	/	/	/	/	/
20	1.5496	1.0026	2.2108	1.0489	1.0137	1.9803
30	1.5605	1.0072	2.0224	1.0555	1.0100	2.0060
40	1.5555	1.0066	2.0176	1.0469	1.0072	2.0083
50	1.5499	1.0056	2.0143	1.0395	1.0056	2.0080
60	1.5451	1.0049	2.0119	1.0338	1.0045	2.0072

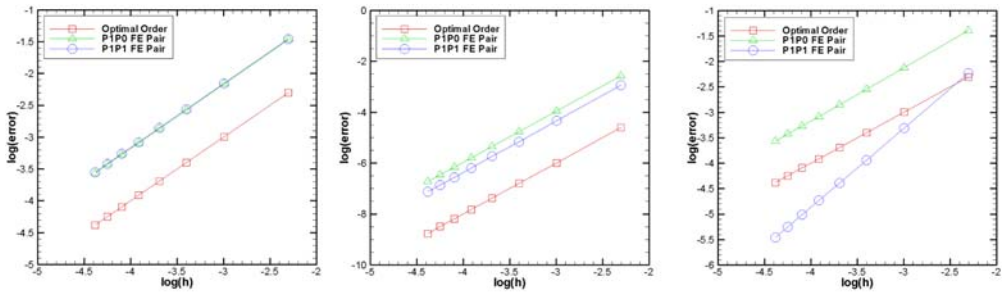

FIG. 2. (a) H^1 convergence order for the velocity, (b) L^2 convergence order for the velocity, (c) L^2 convergence order for the pressure. [Color figure can be viewed in the online issue, which is available at wileyonlinelibrary.com.]

Moreover, by the nonlinear boundary conditions (1.2), the position function g can be chosen as $g = -\sigma_\tau \geq 0$ on each slip boundary Γ_S. Let the initial value $\lambda^1 = 1$ and the parameter $\rho = \nu$. In Table I, we display the relative errors $\frac{\|p-p_h\|_0}{\|p\|_0}$, $\frac{\|\nabla(\mathbf{u}-\mathbf{u}_h)\|_0}{\|\nabla\mathbf{u}\|_0}$, and $\frac{\|\mathbf{u}-\mathbf{u}_h\|_0}{\|\mathbf{u}\|_0}$. Table II intuitively shows the orders of convergence which are consistent with the theoretical estimates obtained in Section IV. The relative L^2 and H^1 convergence rates are displayed in Fig. 2. From the gained results, we can find that numerical tests completely agree with our theoretical analysis.

B. The Backward Facing Step Flow

We test another benchmark problem to demonstrate the stability and efficiency of our methods: the backward facing step problem, which is known to possess a corner singularity. The geometry

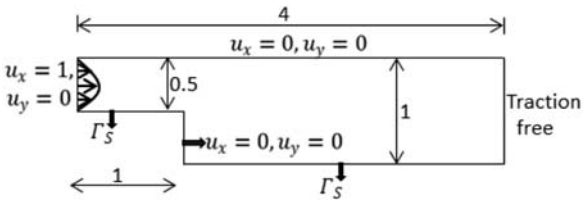

FIG. 3. Computational domain.

and the boundary conditions are shown in Fig. 3 [29]. For this problem, the bottom computational boundary is imposed with the nonlinear slip boundary conditions. In addition, on the upper computational boundary, the inflow section, the outlet boundary and the vertical boundary of the step, a uniform free-stream velocity boundary condition is imposed as shown in Fig. 3. We choose the Reynolds number as 150 based on the maximum velocity $u_x = 1$ at the inlet boundary and the height of the step $l (l = 0.5$ here): $\mathrm{Re} = \frac{u_x l}{\nu}$. The two stabilized finite element pairs are used and $\rho = \nu$ as aforesaid. The mesh is composed of 3044 triangular elements for the velocity in Fig. 4, but for the pressure contour, we select four times finer grids to get a better approximation and keep the same subdivision of the two kinds of finite element pairs. Furthermore, the pressure contour for the $\mathbf{P}_1 - P_0$ finite element pair is fitted by discontinuous points as the piecewise constant space P_0 is adopted for pressure p. The results indicate that the corner causes oscillation, and when fluid flow is downward through the step, eddies are generated though the existence of a slip boundary which can lead to a low-speed region at the horizontal bottom. The pressure contours generated by the two stabilized finite element pairs can be in agreement with the conclusions published in [29].

C. Numerical Simulation of a Blood Flow Model

In this test, we study the influence of blood flow to intravascular thrombosis which considers the bending and bifurcation of two common vascular structures in human body (see [30]). Assume that the blood flow is viscous Newtonian flow, and its governing equations are the incompressible Navier–Stokes equations. We select the same diameter between the bifurcating blood vessels and the main blood vessel with $D = 5$ in a dimensionless scale, the length of horizontal entrance is $4D$, the bending blood vessel is a quarter of the circular arc whose radius is $4D$, and the length of the vertical export branch is $5D$. The angle between the vertical branch and the lateral branch is 45° and the lowest points of the two branches are in the same horizontal plane, which is shown in Fig. 5.

We adopt a constant velocity for the horizontal inlet: $u_x = 0.1$, 1.0, and 2.0, respectively. Numerical calculations ignore the vascular elasticity and permeability for convenience. The nonlinear slip boundary Γ_s has been identified in Fig. 6, and the remaining boundaries are imposed with the Dirichlet boundary conditions excluding the inlet and outlet boundaries. We choose $\nu = 0.01$ and $\rho = \nu$ and apply the stabilized lower-order finite element pairs under the same mesh generation here. Figures 6 and 8 represent the velocity contours of the bifurcating area for clearness, and the streamlines of velocity are shown in Figs. 7 and 9. Preliminary exploratory results show that there exits tangential velocity along the vascular walls on the slip boundary which can impact the vascular sclerosis in human body; Furthermore, the inside wall of the lateral bifurcating blood vessels is easier to form clots. At the beginning, when the inlet velocity in the main blood vessels

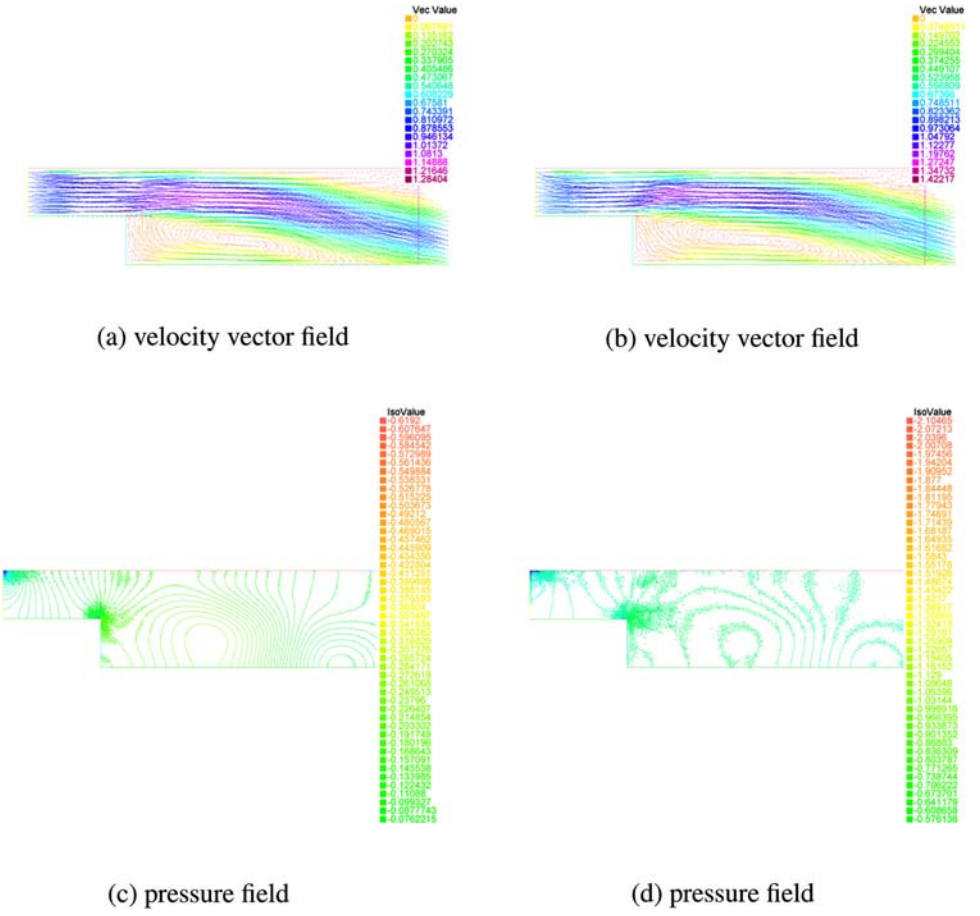

(a) velocity vector field (b) velocity vector field

(c) pressure field (d) pressure field

FIG. 4. The velocity vector and pressure fields under different finite element pairs: $\mathbf{P}_1 - P_1$ (left) and $\mathbf{P}_1 - P_0$ (right). [Color figure can be viewed in the online issue, which is available at wileyonlinelibrary.com.]

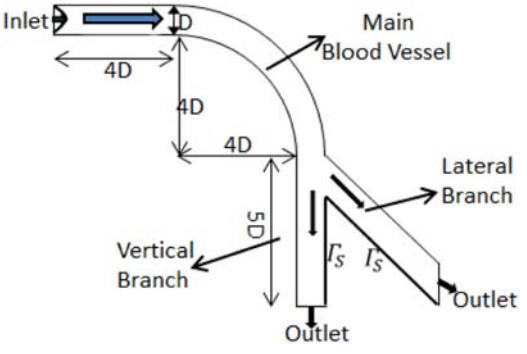

FIG. 5. Computational domain. [Color figure can be viewed in the online issue, which is available at wileyonlinelibrary.com.]

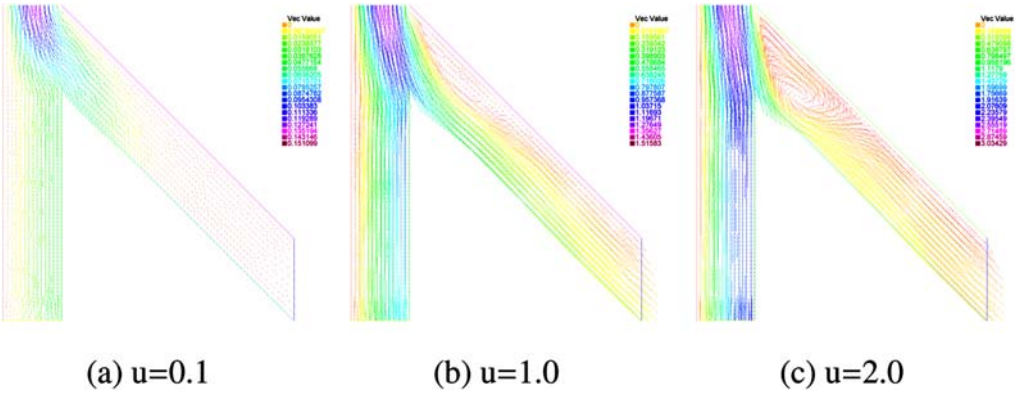

FIG. 6. Velocity contours of bifurcate area with different initial inlet velocity under stabilized $\mathbf{P}_1 - P_1$ pair. [Color figure can be viewed in the online issue, which is available at wileyonlinelibrary.com.]

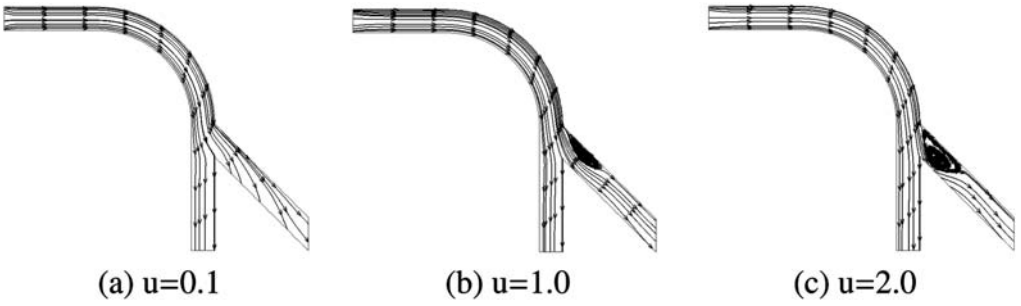

FIG. 7. Streamline contours with different initial inlet velocity under stabilized $\mathbf{P}_1 - P_1$ pair.

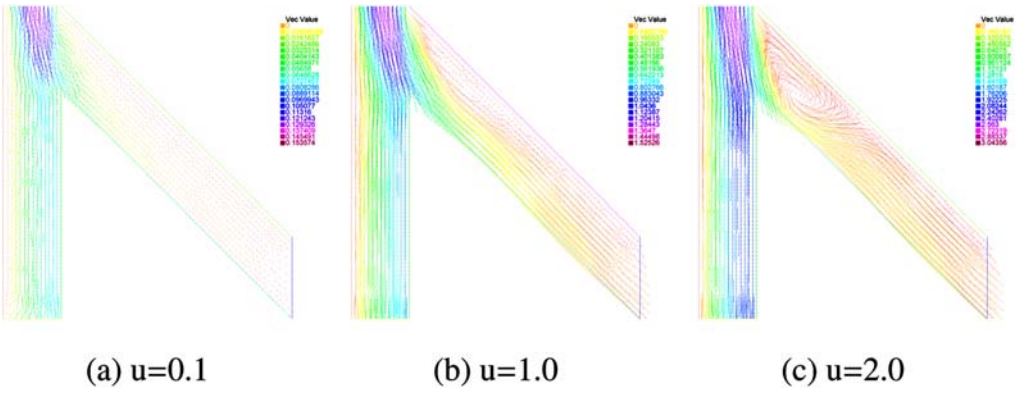

FIG. 8. Velocity contours of bifurcate area with different initial inlet velocity under stabilized $\mathbf{P}_1 - P_0$ pair. [Color figure can be viewed in the online issue, which is available at wileyonlinelibrary.com.]

is small, the flow in the bifurcating blood vessels is smooth, with an increase of the inlet velocity, the outside of the lateral bifurcating vessel starts to form eddies, and the bigger the inlet velocity, the more strength and the lager range of the eddies, which lead to a greater chance of thrombosis around the corner (Figs. 7 and 9).

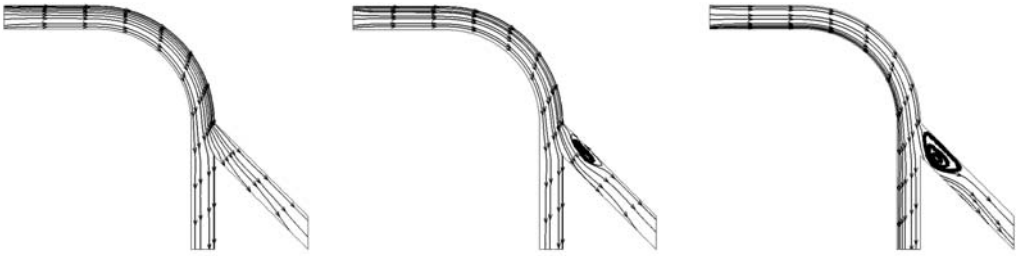

FIG. 9. Streamline contours with different initial inlet velocity under stabilized $\mathbf{P}_1 - P_0$ pair.

VI. CONCLUSIONS

In this work, we have provided a theoretical analysis for the stabilized finite element methods for a blood flow model of arteriosclerosis, which is governed by the incompressible Navier–Stokes equations with nonlinear slip boundary conditions. Based on the framework of the finite element method for the linear Stokes flow with slip or leak boundary conditions of the friction type in [6, 7], we have studied the nonlinear Naveir–Stokes problem with the slip boundary conditions. Optimal estimates are obtained for the lower-order finite element pairs $\mathbf{P}_1 - P_1$ and $\mathbf{P}_1 - P_0$. The results of an analytical solution example and the backward facing step flow problem demonstrate that our presented methods are stable and efficient. Meanwhile, the simulation of a blood flow model displays the formation of thrombosis in the blood vessels of human body. In summary, the numerical tests performed are consistent with the theoretical results established.

References

1. H. Fujita, Flow problems with unilateral boundary conditions, College de France, Lecons, 1993.
2. H. Fujita, A mathematical analysis of motions of viscous incompressible fluid under leak or slip boundary conditions, RIMS Kokyuroku 888 (1994), 199–216.
3. N. Saito, On the Stokes equations with the leak and slip boundary conditions of friction type: regularity of solutions, Publ RIMS, Kyoto Univ 40 (2004), 345–383.
4. Y. Li and K. T. Li, Pressure projection stabilized finite element method for Navier-Stokes equations with nonlinear slip boundary conditions, Computing 87 (2010), 113–133.
5. Y. Li and K. T. Li, Uzawa iteration method for Stokes type variational inequality of the second kind, Acta Math Appl Sin 17 (2011), 303–316.
6. T. Kashiwabara, On a finite element approximation of the Stokes equations under a slip boundary condition of the friction type, Jpn J Ind Appl Math 30 (2013), 227–261.
7. T. Kashiwabara, Finite element method for Stokes equations under leak boundary condition of friction type, SIAM J Numer Anal 51 (2013), 2448–2469.
8. R. An and Y. Li, Two-level penalty finite element methods for Navier-Stokes equations with nonlinear slip boundary conditions, Int J Numer Anal Model 11 (2014), 608–623.
9. R. An and X. Wang, Two-level Brezzi-Pitkaranta discretization method based on Newton iteration for Navier-Stokes equations with friction boundary conditions, Abstr Appl Anal (2014).
10. X. X. Dai, P. P. Tang, and M. H. Wu, Analysis of an iterative penalty method for Navier-Stokes equations with nonlinear slip boundary conditions, Int J Numer Meth Fluids 72 (2013), 403–413.

11. J. K. Djoko, On the time approximation of the Stokes equations with slip boundary condition, Int J Numer Anal Model 11 (2014), 34–53.
12. H. Fujita, Non-stationary Stokes flows under leak boundary conditions of friction type, J Comput Math 19 (2001), 1–8.
13. H. Fujita, A coherent analysis of Stokes flows under boundary conditions of friction type, J Comput Appl Math 149 (2002), 57–69.
14. H. Fujita and H. Kawarada, Variational inequalities for the Stokes equation with boundary conditions of friction type, Int Ser Math Sci Appl 11 (1998), 15–33.
15. T. Kashiwabara, On a strong solution of the non-stationary Navier-Stokes equations under slip or leak boundary conditions of friction type, J Differ Equ 254 (2013), 756–778.
16. Y. Li and R. An, Two-level pressure projection finite element methods for Navier-Stokes equations with nonlinear slip boundary conditions, Appl Numer Math 61 (2011), 285–297.
17. Y. Li and K. T. Li, Existence of the solution to stationary Navier-Stokes equations with nonlinear slip boundary conditions, J Math Anal Appl 381 (2011), 1–9.
18. Y. Li and R. An, Semi-discrete stabilized finite element methods for Navier-Stokes equations with nonlinear slip boundary conditions based on regularization procedure, Numer Math 117 (2011), 1–36.
19. N. Saito and H. Fujita, Regularity of solutions to the Stokes equation under a certain nonlinear boundary condition, Lect Notes Pure Appl Math 223 (2002), 73–86.
20. R. A. Adams, Sobolev spaces, Academic Press, New York, 1975.
21. V. Girault and P. A. Raviart, Finite element method for Navier-Stokes equations: theory and algorithms, Springer-Verlag, Berlin, Heidelberg, 1986.
22. R. Temam, Navier-Stokes equations, theory and numerical analysis, 3rd Ed., North-Holland, Amsterdam, 1983.
23. H. Fujita, H. Kawarada, and A. Sasamoto, Analysis and numerical approaches to stationary flow problms wth leak and slip boundary conditions, Lect Notes Numer Appl Anal 14 (1995), 17–31.
24. Z. X. Chen, Finite element methods and their applications, Springer-Verlag, Heidelberg, New York, 2005.
25. P. B. Bochev, C. R. Dohrmann, and M. D. Gunzburger, Stabilization of low-order mixed finite elements for the stokes equations, SIAM J Numer Anal 44 (2006), 82–101.
26. J. Li and Y. N. He, A stabilized finite element method based on two local Gauss integrations for the Stokes equations, J Comput Appl Math 214 (2008), 58–65.
27. R. Glowinski, J. Lions, and R. Tremolieres, Numerical analysis of variational inequalities, Springer, North-Holland, 1981.
28. Y. N. He and J. Li, Convergence of three iterative methods based on the finite element discretization for the stationary Navier-Stokes equations, Comput Methods Appl Mech Eng 198 (2009), 1351–1359.
29. L. P. Franca and A. Nesliturk, On a two-level finite element method for the incompressible Navier-Stokes equations, Int J Numer Methods Eng 52 (2001), 433–453.
30. L. L. Xiong and H. A. Ma, Numerical simulation of non-Newtonian blood flow in a three dimensional complex blood vessel, Chin J Med Guide 13 (2011), 303–307.